ISBN: 978-3-95450-261-5 ISSN: 2673-7000 doi: 10.18429/JACoW-NAPAC2025-WEP011

ANALYSIS OF VAPOR DIFFUSION Nb_3Sn COATING AT FERMILAB: MINIMIZING IMPURITIES USING TOF-SIMS

N. Tagdulang*, B. Tennis, D. Bafia, J. Lee, S. Posen, G. Eremeev
Fermi National Accelerator Laboratory, Batavia, IL, USA
T. Peterson, M. Kelly, Argonne National Laboratory, Argonne, IL, USA

Abstract

Nb_3Sn demonstrates steady advancements offering reduced power cost in superconducting radio-frequency cavities due to its high critical temperature, quality factor, and achieved accelerating gradient. However, theoretical estimates of its radio-frequency parameters have not been achieved due to several potentially limiting mechanisms: tin spots, patchy regions, defects, thermal impedance, and impurities. While some of these limitations have been intensively studied, impurity analysis in Nb_3Sn coatings has received less attention. We report an investigation of impurities in several vapor-diffused Nb_3Sn coated samples using time-of-flight secondary ion mass spectroscopy (TOF-SIMS) and show allowable impurity levels in view of superconducting cavity performance. Challenges and lessons learned in maintaining clean Nb_3Sn coatings are also discussed.

INTRODUCTION

Nb_3Sn superconducting radio frequency (SRF) cavities have been extensively studied due to their promising superconducting properties, theoretically, they far surpasses the current state-of-the-art Nb cavities. The Nb_3Sn cavities could reach superconducting transition (T_c) and superheating field (H_{sh}) both twice as high as that of Nb, while having an unloaded quality factor (Q_0) at 4 K comparable or higher to that of Nb at 2 K. Such cavities, therefore, theoretically, can reach accelerating gradient (E_{acc}) to roughly 100 MV/m in standard 1.3 GHz Tesla cavity [1]. These predicted properties not only provide an avenue for frontier research of linear accelerators, but also reduce cryogenic and capital costs. Hence, this is currently being pursued in many research groups around the world, both for basic research studies and industrial applications [2–6].

The vapor diffusion method is presently the leading technique to deposit Nb_3Sn on SRF cavities. Primarily, it involves two steps of heating: at 500 °C where $SnCl_2$ evaporates and is allowed to nucleate on the substrate, and at 1100 °C where the Sn coating and annealing are enabled. However, the best Nb_3Sn-coated cavity to date has achieved an accelerating gradient of $E_{acc,max} = 24$ MV/m ($B_{pk,max} = 95$ mT), less than that of the well-performed Nb cavities. Moreover, the reproducibility of this coating remains a challenge. These can be attributed to any or a combination of the following reasons: unreacted Sn spots, patchy regions, thermal impedance, surface roughness, cracking of the Nb_3Sn coating, substrate dependence, and impurities [1, 2, 4, 7, 8].

* ntagdula@fnal.gov

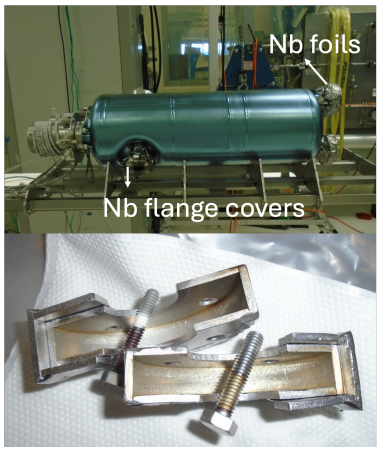

Figure 1: Top: QWR 145 prepared for Nb_3Sn coating. Bottom: A photograph of a flange cover after the coating process.

There are continued studies aimed at understanding each of these effects. However, although the effect of Ti as impurity was assumed to be the cause of some degraded coatings performance at JLAB [9], there are only a few studies performed on the effect of impurities on cavity RF performance.

Figure 1, at the top, shows QWR 145 cavity, sitting on the Nb frame. As seen in the figure, the NbTi flanges were covered with flange covers made of Nb to minimize the diffusion of Ti during coating. In addition, they were covered with Nb foils for further security. The bottom of the figure depicts a Nb flange cover after a Nb_3Sn coating; one can see an obvious discoloration. These coatings provide us with the opportunity to explore the effect of Ti on Nb_3Sn-coated cavities. This contribution, therefore, is our first attempt to rationalize the effect of Ti on cavity performance in the same coating chamber. Moreover, we show what other impurities are found on the Nb_3Sn coated samples and how we minimized them using TOF-SIMS.

THE Nb_3Sn SAMPLES AND CAVITY RF PERFORMANCE

The cavities used in this study are B9AS-AES-002, QWR 218, and QWR 145 as listed in Table 1. The corresponding frequencies are also listed. We specify B9AS-AES-002 as the baseline, since many cavities coated in Fermilab showed common performance. It can be seen that QWR 145 achieved the highest maximum peak magnetic field of $B_{pk,max} = 100$ mT with the lowest surface resistance. To our knowledge, this is the best achieved so far in Nb_3Sn. This is followed by QWR 218, with $B_{pk,max} = 74$ mT, higher than

ISBN: 978-3-95450-261-5 ISSN: 2673-7000 doi: 10.18429/JACoW-NAPAC2025-WEP011

Table 1: Maximum Peak Magnetic Field $B_{pk,max}$, and Surface Resistance at $B_{pk,max}$, $R_{s,max}$, as Obtained During the VTS Measurements

Cavities	f [MHz]	$B_{pk,max}$ [mT]	$R_{s,max}$ [nΩ]
B9AS-AES-002 (Baseline)	650	62	66
QWR 218	218	74	155
QWR 145	145	100	63

the $B_{pk,max}$ = 62 mT of baseline. Although the $B_{pk,max}$ is higher in QWR 218 compared to baseline, the surface resistance is more than twice as high, albeit lower in frequency.

The Nb_3Sn witness samples used in this study were coated at the same time as the cavities. In some of them, the samples were placed in a small slot in the source tube. In our coatings, we often leave the other end of the cavity open. At this open end, we also hung a witness sample.

Figure 2 presents the scanning electron microscope (SEM) images of the Nb_3Sn-coated samples. The baseline sample has the highest grain size of about 1.8 µm. QWR 145 shows the smallest grain size in both its samples. It is worth highlighting that both samples in QWR 145 achieved a similar grain size of about 0.8 µm, suggesting homogeneous and uniform coating across the cavity. We believe that this may be the reason for the unprecedented cavity performance of this cavity discussed above, although having lower frequency compared to baseline is also a factor. In contrast, the grain size of the QWR 218 samples varies largely from 1.6 µm (source end) to 0.6 µm (open end).

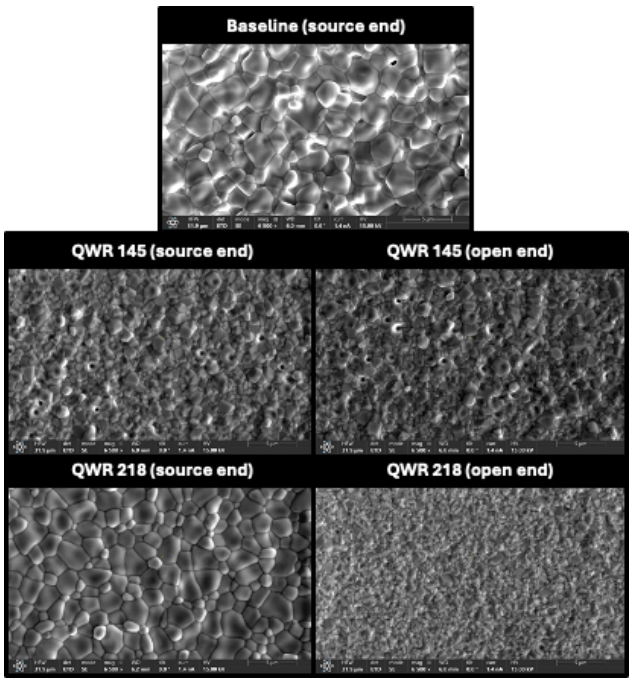

Figure 2: SEM images of Nb_3Sn-coated witness samples from cavity runs, all on the same scale. Source end and open end indicate samples placed inside the source tube and hanging at the end of the cavity left open in the coating chamber, respectively.

IMPURITIES

We used TOF-SIMS to analyze the impurities in the Nb_3Sn samples based on their charge to mass ratio (m/z). An O_2+ sputter ion source with 2 keV beam energy was used to detect positive secondary ions. On the other hand, Cs+ sputter ion source with 2 keV current was used to measure negative secondary ions. We used 600 x 600 µm sputter crater and 200 x 200 µm analysis area. In each sample, data were obtained in three spots and were used to calculate the uncertainty and show repeatability of the depth profile. To save time and resources, only one measurement was performed across the Nb_3Sn layer.

Figure 3 shows the cross-section of the QWR 145 (source end) sample. It can be seen that the Nb_3Sn layer has a thickness of about 1.5 µm. In our analysis, we used this thickness to calibrate the sputter rate, giving 0.3 nm/s and 0.2 nm/s for O_2+ and Cs+ sputter sources, respectively.

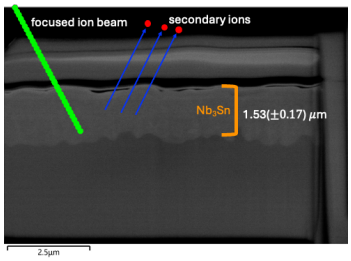

Figure 3: Cross-section of QWR 145 sample (source end) showing Nb_3Sn thickness of about 1.53 µm.

In our analysis of the mass spectrum, we found traces of Ti+, Si+, Al+, Na+, K+, Ca+, In+, F-, Cl-, O-, H-, and C-. While the effect of all these impurities is unknown, this study focuses on Ti, which was one of the assumed impurities that can cause quality factor degradation in Nb_3Sn-coated SRF cavities [9].

Figure 4 (top) shows the depth profile of Ti in all samples studied. The Ti diffused to about 1.5 µm. It is clear that the QWR 145 located at the source has the highest amount of Ti, depicted also in the integrated counts as shown in the bottom figure. It is worth mentioning that only traces of Ti were found since it was not detected or close to the detection limit of X-ray photoelectron spectroscopy. The sample at the open end of the cavity has a smaller amount of Ti. This suggests that the flanges at the open end are well covered than at the source end, and/or the Ti diffusion from the source didn't reach strongly towards the end of the cavity. Nonetheless, both of these samples demonstrate higher integrated counts of Ti compared to baseline. As described in the previous

ISBN: 978-3-95450-261-5 ISSN: 2673-7000 doi: 10.18429/JACoW-NAPAC2025-WEP011

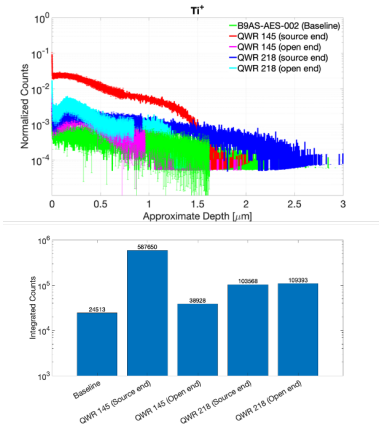

Figure 4: Top: Depth profile of Ti^+ in the Nb_3Sn samples normalized with that of the Nb^+ counts. Bottom: Integrated counts of Ti.

section, the QWR 145 cavity showed better performance than baseline, suggesting that this level of Ti, at least to the sample at the open end close to where the surface magnetic field is at its highest, does not degrade cavity performance. Differently, both QWR 218 samples showed nearly the same amount of integrated counts, higher than the baseline and QWR 145 (open end). QWR 218 has achieved $B_{pk,max}$, higher than baseline. Hence, this amount of Ti may not be detrimental to achieving a higher $B_{pk,max}$ than baseline, but the surface resistance is significantly high. We may speculate from these data that the high surface resistance in QWR 218 may be due to Ti. However, this can also be from the inhomogeneous coating of this cavity based on the SEM images in Fig. 2.

DECONTAMINATION OF COATING CHAMBER AND COMPONENTS

Burnout is the method typically used to decontaminate furnaces. This is usually done at the highest allowed operating temperature of the furnace. To decontaminate our coating chamber and coating components, we performed successive burnout at 1200 °C for 3h. Although we focused on correlating RF performance with the amount of Ti in the Nb_3Sn samples, when decontaminating the coating chamber, we were looking at minimizing all the contaminants as much as possible. In addition to Ti+, the dominant contaminant is Si+.

Figure 5 shows the integrated counts of Ti+ and Si+. The succession of burnouts contains the following components: 11/21/24 coating chamber, 01/23/25 same as 11/21/24, 01/25/25 two source tubes, frame, and all thermocouples, 02/11/25 same as 01/25/25, and 012/14/25 one source tube + frame. These are compared with an untreated electropolished (EP) Nb sample. It can be seen from 11/21/24 and 01/23/25 that the consecutive burnout decreased the Ti+ counts. However, they still remain higher than EP Nb. This suggests a substantial amount of Ti+ in the coating chamber. Introducing all the components used for coating, the Ti count is increased, indicating that these contaminants have

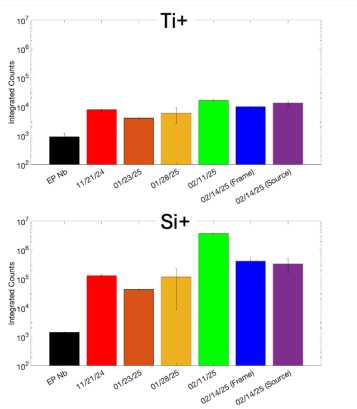

Figure 5: Integrated counts of Ti (top) and Si(bottom) from series of burnouts.

some level of Ti+ also. The same burnout was performed on 02/11/25 and found that the Ti counts increased further. These results suggest that Ti+ cannot be burned out and that we have a continuous source of it, probably accumulated over time. This is evident by the fact that even though we remove some components during the burnout on 02/14/25, the counts of Ti remain higher compared to those in 02/11/25. We find the same results for Si+. It is worth noting that between the samples located on the frame and on the source in 02/14/25, the integrated counts are within the uncertainty, indicating that the effect of the sample position is negligible.

The above study suggests that the burnout method is not effective in decontaminating the coating chamber and components. We performed buffered chemical polishing to remove some microns of the surface instead. We checked the quality of the surface removal by performing another burnout on the coating chamber and found a level of impurities comparable to EP Nb.

SUMMARY AND CONCLUSION

We showed the level of Ti found in Nb_3Sn witness samples coated alongside SRF cavities. We found that Ti diffused to about 1.5 µm deep. QWR 145 cavities achieved the best performance so far in Nb_3Sn, although it has a higher Ti level than that of the baseline. This study sets allowable Ti level for SRF cavities, especially those with NbTi flanges.

We also performed successive burnout and have analyzed the effectiveness of the method to decontaminate the coating chamber and components. We find that it is not effective for removing Ti and Si. This study is a step forward in understanding the effect of impurities and possibly improving reproducibility in Nb_3Sn across different furnaces.

ACKNOWLEDGEMENTS

This work was produced by FermiForward Discovery Group, LLC under Contract No. 89243024CSC000002 with the U.S. Department of Energy, Office of Science, Office of High Energy Physics. N. Tagdulang would like to acknowledge Wieslawa Dziedzic-Misiewicz and Adam Clairmont for their support in the materials characterization of the samples studied.

ISBN: 978-3-95450-261-5 ISSN: 2673-7000 doi: 10.18429/JACoW-NAPAC2025-WEP011

REFERENCES

[1] E. Viklund, D. N. Seidman, D. Burk, and S. Posen, "Improving Nb_3Sn cavity performance using centrifugal barrel polishing," *Supercond. Sci. Technol.*, vol. 37, no. 2, p. 025009, 2024.

[2] G. V. Eremeev, U. Pudasaini, S. Cheban, G. Ciovati, M. Drury, J. Fischer, K. Macha, M. McCaughan, A. Reilly, R. Rimmer *et al.*, "Demonstration of E_{acc}= 10 MV/m with Nb_3Sn cavities in a cryomodule," *Supercond. Sci. Technol.*, 2024.

[3] R. Dhuley, S. Posen, M. Geelhoed, O. Prokofiev, and J. Thangaraj, "First demonstration of a cryocooler conduction cooled superconducting radio-frequency cavity operating at practical CW accelerating gradients," *Supercond. Sci. Technol.*, vol. 33, no. 6, p. 06LT01, 2020.

[4] S. Posen, J. Lee, D. N. Seidman, A. Romanenko, B. Tennis, O. Melnychuk, and D. Sergatskov, "Advances in Nb_3Sn superconducting radio-frequency cavities towards first practical accelerator applications," *Supercond. Sci. Technol.*, vol. 34, no. 2, p. 025007, 2021.

[5] T. K. Kroc, "Motivation and development of a compact superconducting accelerator for X-ray medical device sterilization," 2021. doi:10.48550/arXiv.2112.07553

[6] I. Gonin, S. Kazakov, R. Kephart, T. Khabiboulline, T. Nicol, N. Solyak, J. Thangaraj, and V. Yakovlev, "Built-in thermionic electron source for an SRF linacs," Fermi National Accelerator Lab.(FNAL), Batavia, IL, USA, Tech. Rep., 2021.

[7] S. Posen *et al.*, "Cutout Study of a Nb3Sn Cavity", in *Proc. SRF'15*, Whistler, Canada, Sep. 2015, paper TUPB049, pp. 681–685.

[8] S. A. Willson, A. V. Harbick, L. Shpani, V. Do, H. Lew-Kiedrowska, M. U. Liepe, M. K. Transtrum, and S. Sibener, "Impact of sub-micron Nb_3Sn stoichiometric surface defects on high-field superconducting radiofrequency cavity performance," *Phys. Rev. Res.*, vol. 6, no. 4, p. 043133, 2024.

[9] U. Pudasaini, M. J. Kelley, G. V. Eremeev, C. E. Reece, and J. Tuggle, "Surface Studies of Nb3Sn Coated Samples Prepared under Different Coating Conditions,"in *Proc. SRF'17*, Lanzhou, China, Jul. 2017, pp. 894–899. doi:10.18429/JACoW-SRF2017-THPB069